Sustainable Energy, 2017, Vol. 5, No. 1, 16-25
Available online at http://pubs.sciepub.com/rse/5/1/3

DOI:10.12691/rse-5-1-3

Photovoltaic Cell String Layout

João Paulo N. Torres*, Carlos Alberto Fernandes, João C. Leite

Instituto de Telecomunicações, Instituto Superior Técnico, Universidade de Lisboa, Lisboa, Portugal
*Corresponding author:

Abstract The aim of this work is to evaluate possible ways of minimizing the effect of both the longitudinal and transversal shading properties inherent to concentrating collectors that are fixed to building structures. Solarus AB PVT cell strings contain 38 solar cells connected in series. Solar cells in the concentrated side of the collector are shaded due to the presence of the aluminium frame of the PVT collector. The effects of shading and of non-uniform illumination are minimized by including bypass diodes. Each string has 4 groups of bridged cells, each one associated to a bypass diode. In this work, different combinations of string cells in the collector receiver have been simulated in a LTPSPICE environment. At the end, a comparative analysis is presented.

Keywords: *solar cells, longitudinal and transversal shading, concentrating collectors, bypass diodes*

Cite This Article: João Paulo N. Torres, Carlos Alberto Fernandes, and João C. Leite, "Photovoltaic Cell String Layout." *Sustainable Energy*, vol. 5, no. 1 (2017): 16-25. doi: 10.12691/rse-5-1-3.

1. Introduction

As the effects of climate change are becoming increasingly obvious and the global oil reserves seem to have reached their peak production, a change in the energy system is becoming necessary. Improving the existing resources, on one hand, and searching for alternative sources, on the other hand, appear to be the appropriate strategy. Efficient and economic harnessing of clean solar power may be very significant for fulfilling today's growing energy needs and tranquilizing climate concerns. Solar power can be solar photovoltaic (PV), solar thermal and hybrid of solar photovoltaic and thermal (PVT) [1]. Solar energy has the advantage of being environmental friendly, and have unlimited availability [2]. PV energy is highly dependent on the environmental conditions, such as temperature and solar irradiation, which makes the optimization analysis rather complex [3].

Stationary solar concentrating hybrid PVT systems use reflectors, which may cause non uniform distribution of light on the string of PV cells. Similarly, partial shading creates non-uniform illumination and, hence, the developments of hot spots in solar PV module, which may cause permanent damage to the cells that are shaded. Partial shading has a larger impact on the PV efficiency (electrical energy output of PVT collectors) than on the thermal efficiency (thermal energy output of PVT collectors).

1.1. Work Goals

The work is intended to evaluate possible alternatives for the most usual cell string layout and the bypass diode configuration, in order to minimize the effects of non-uniform illumination and shading inherent to stationary concentrating collectors. The simulation is carried in an LTSPICE[1] software to model the string of solar cells and bypass diodes.

The document is organized as per the following:

- Section 1 is a general introduction of the work and describes the fundamentals of solar energy;
- Section 2 is a description of the state of the art of concentrating solar hybrid PVT collectors;
- Section 3 describes briefly Solarus AB Compound Concentrating Collectors;
- Section 4 describes in detail solar cell modelling and simulation for the analysis of the shading effects in strings of solar cells;
- Section 5 presents the simulation results of the models described in section 4, taking into account the data obtained from Solarus AB, when different configurations of solar cell strings are considered;
- Section 6 makes a summary of the conclusions, recommendations and future work.

1.2. Solar Radiation

Solar energy is a term related to part of the sun's electromagnetic energy converted to useful electrical or thermal energy on earth. Solar radiation is an electromagnetic wave emitted by the sun. The total power density of the solar radiation at the mean earth-sun distance, on a plane perpendicular to the direction of the sun outside the earth's atmosphere, is referred to as the *solar constant* [4]. Solar constant is the intensity of solar irradiation directly outside the earth's atmosphere on a horizontal surface. It is almost constant at around 1367W/m^2. This value is annual averaged because the solar radiation varies slightly over the year due to the earth's slightly elliptical orbit around the sun and the solar

[1] Electronic circuits simulator, Linear Technology Simulation Program for Integrated Circuits Emphasis.

activity is not constant. The solar radiation that reaches the earth's surface is only 1000W/m^2.

As the latitude of the place on earth increases, the solar irradiance that falls on that particular place decreases. This is due to the increase in the angle of incidence of solar radiation at higher latitude. As a consequence, the average irradiance at high latitude is lower than places at lower latitude. The different spectra in Figure 1 refer to the black-body radiation at 6000K, the extraterrestrial AM0 radiation and the AM1.5 [2] radiation. The earth receives both direct and diffuse sunlight.

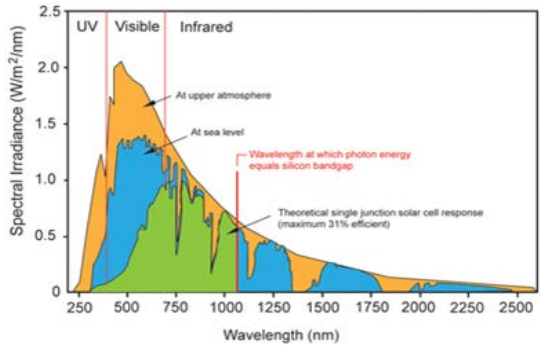

Figure 1. Spectral power density of sunlight

The total ground radiation is called the *global radiation*. The portions of these two components depend on weather conditions in a particular instant. In general, the solar radiation that strikes the earth per square meter depends on the day of the year, time of the day and latitude.

1.3. Photovoltaic Effect

The working principle of solar cells is based on the *photovoltaic effect*.

If the photon energy is greater or equal to the energy band gap of the semiconductor material, it will give rise to the creation of electron-hole pair. This determines the minimum frequency for the light to be absorbed by the material, regardless of its intensity. If an external load is connected across the *p-n* junction, the electrons move through the external circuit and recombines with the holes, producing an electric current.

2. State of the Art

Concentrating collectors use optical devices, such as mirrors/aluminium or lenses, to concentrate light to the receiver in order to increase the light collected by the device.

The concentration of solar radiation into the receiver increases the intensity of radiation and, consequently, the collected power. In the case of photovoltaic collectors, concentrating the rays may cause non-uniform illumination and thermal overheating on PV cells. In solar PVT collectors it is possible to obtain both thermal and electrical energy from the same collector. Avoiding the increase of the temperature, the hybrid collectors have an additional advantage in the efficiency when compared to the PV collectors.

Solarus Compound Parabolic Collector

Solarus Compound Parabolic Concentrator (CPC) is a non imaging concentrating collector. These stationary collectors operate without tracking system.

In electrical or thermal energy outputs from solar PVT collectors, the photovoltaic and thermal absorbers are expensive. The use of concentrating collectors minimizes the collector area, by replacing the costly absorber by inexpensive reflective materials, and so a reduction in the overall costs become possible. For concentrated PV solutions, it is necessary to remove the built up heat from the PV cell, According to Gomes et. al [5], the main advantages of PVT collectors, when compared to PV and solar thermal collectors, are:

- a reduction in the lower production cost per KWh of annual of the energy conversion system [5], because PVT uses fewer expensive raw materials than an equivalent area of thermal and PV panels;.
- higher efficiencies due to a lower temperature of operation. This is ensured by the cooling obtained by water that circulates in the pipes of thermal absorber;
- longer life time of the solar cells of the PVT;
- a reduction in the installation area (especially important when the available space is limited, like roofs).

2.1. The Maximum Reflector Collector (MaReCo)

Basically, the MaReCo (Figure 2) consists of an asymmetrical truncated CPC with a flat receiver, preferably bi-facial absorbers in order to minimize the absorber area. The main purpose of the MaReCo is to optimize the annual performance for a given reflector area, by reducing the expensive absorber area with the use of less expensive reflectors, which also minimizes the heat losses [6].

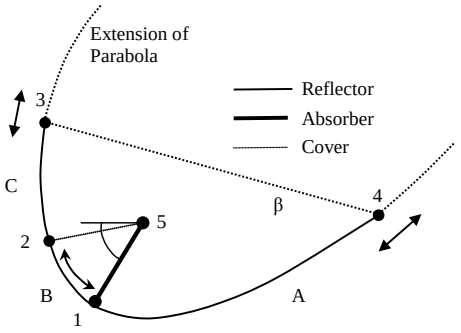

Figure 2. basic MaReCo design [7]

Some details about the MaReCo designs are given in the following:

Part A: Section 1–4, which is the lower parabolic reflector.

[2] The spectrum outside the atmosphere (approximated by the 5,800 K black body) is referred to as "AM0", meaning "zero atmospheres". Solar cells used for space power applications are generally characterized using AM0. The spectrum after travelling through the atmosphere to sea level with the sun directly overhead is referred to as "AM1". Solar panels do not generally operate under exactly one atmosphere's thickness. An effective thickness shall be used to take into account with the angle of the sun regarding the Earth's surface. Since the major population centres lie in temperature latitudes, an "AM1.5", 1.5 atmosphere thickness is much more common.

Part B: Section 1–2, whose function is directing light to the absorber.

Part C: Section 2–3, which is the upper parabolic reflector.

The aperture 3–4 is covered by glass. Points 3 and 4 can vary along the extensions of the parabola depending on the desired truncation. The absorber (1–5) makes an angle φ with the horizontal, called the *absorber inclination angle*, and the aperture (3–4) makes an angle β with the horizontal, called the *aperture tilt* [7].

The Roof-Integrated MaReCo

The roof-integrated MaReCo is designed to be mounted directly on south-facing roofs in northern hemisphere, with the glass parallel with the roof surface, and the trough axis parallel to the ground.

2.2. Concentration Factor (C)

Concentration factor represents the ratio of concentrated light to non-concentrated light. Its value for Solarus PVT, with anisotropic light sources (a combination of beam and diffuse light) is given by,

$$C = \frac{\text{Aperture area}}{\text{Receiver area}} \quad (1)$$

The area concentration ratio of the Solarus PVT collector for the lower part of the receiver is given by

$$C = \frac{\text{Aperture area}}{\text{Receiver area}} = \frac{0.273 \times 2.31}{0.158 \times 2.31} = 1.728$$

This gives an average concentration factor of 1.4 to1.5 suns.

3. Solarus PVT Collectors

Solarus PVT Collector (Figure 3) is a compound parabolic collector (CPC).The receiver is placed in one side of the concentration trough instead of at centre, as in symmetric collectors. The receiver is a bi-facial PV pasted in a thermal absorber with pipes in the absorber. The solar radiation is concentrated onto a thermal absorber, from an aluminium reflector. A highly transparent and electrically insulating silicone is used to laminate the PV cells to the thermal absorber on both sides of the absorber.

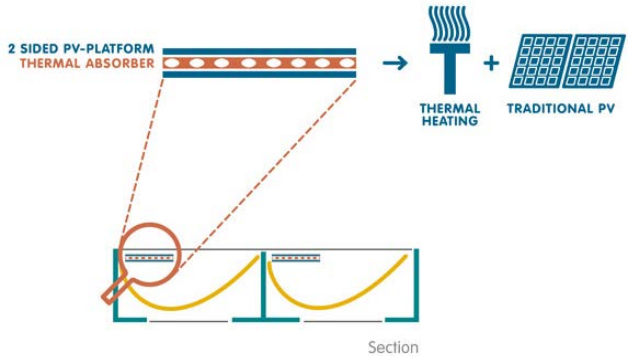

Figure 3. Solarus PVT Collector (side view)

Though the concentration factor of Solarus PVT collector is low, the PV cells can still reach high temperatures. Since mono-crystalline solar cells exhibit a reduction in power output at elevated temperatures, cooling is needed to maintain the electrical efficiency. Cooling is accomplished by running water, through the channels of the thermal absorber. Therefore, the PVT collector produces electricity and heat from the same area.

The optical axis for the reflector geometry is normal to the glass of the collector, which defines the acceptance angles for an effective radiation. If radiation falls outside this angle, the reflector does not redirect the incoming beam radiation to the lower side of the absorber, leading to a strong reduction in the optical efficiency of the collector [8].

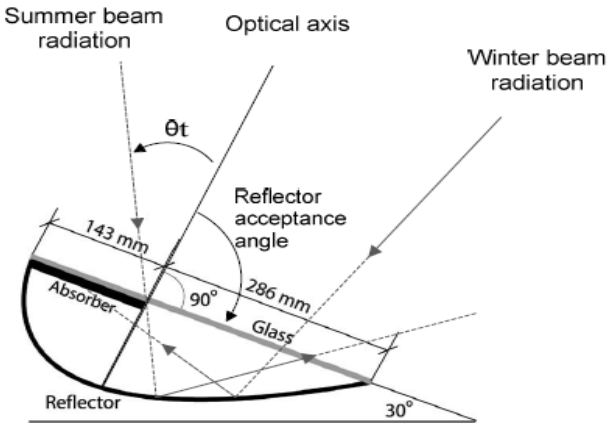

Figure 4. Cross section of CPC Collector

The collector's optical efficiency changes throughout the year, depending on the projected solar altitude. The tilt determines the amount of total annual irradiation kept within the acceptance angle interval [9]. As a result, by varying the tilt, it is possible to increase the effective collector area, without causing overproduction in the summer when the collector has lower optical efficiency.

3.1. Solarus Receiver (Trough)

Figure 5 shows the collector plan view. The PVT collector has two troughs. The water connections for extracting the heat are represented in blue and the electrical arrangements of the solar cells are shown in red. Since both troughs are similar, most tests need only the investigation of a single trough. The lower part of the receiver, i.e., the part that receives concentrated light, has exactly the same hydraulic arrangement and similar electrical configuration. The concentrated side of each trough has 38 solar cells of 1/3[3] type.

In this work the test is carried for a single string of 38 cells with 4 bypass diodes. Each trough has two sides (Figure 6); the concentrated side of the receiver has two identical strings of cells per trough, if the cells are 1/6 cell type, or one string of 38 solar cells, if they are 1/3 cell type

[3] Standard cell has a size of 156mm×156mm, the cell is cut to 148mm×156mm to fit the receiver and then the longer dimension is cut in to three equal solar cells called 1/3 solar cell with a dimension of 52mm×148mm, if these cells are again cut in to two halves they form a cell called 1/6 with dimension 26mm×148mm

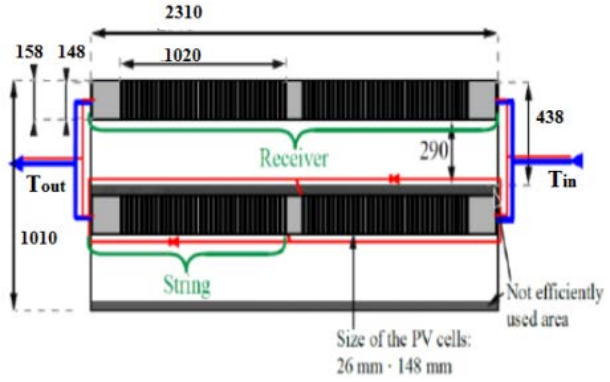

Figure 5. top view [14] (all dimensions are in mm)

3.2. Shading of the PVT

The shade from the frame falls on the reflector and is the main source of shade for the concentrated side.

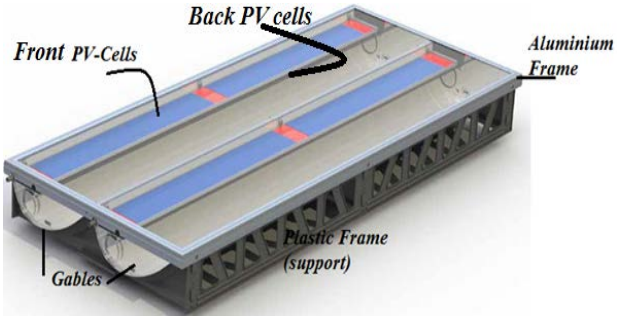

Figure 6. Solarus PVT

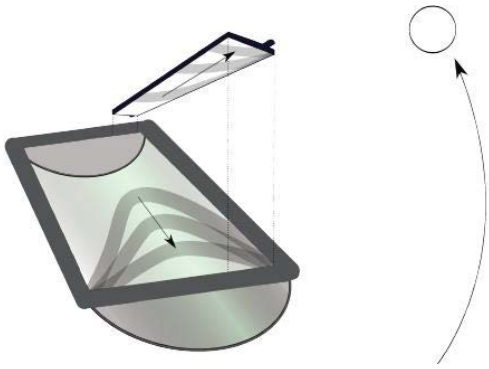

Figure 7. Shading from the frame of PVT

In Figure 7, the arrows show the movement of the shade produced by the frame on the reflector trough and on the underside of the receiver, as the sun rises from the horizon to zenith.

Shading has different impact on PV panels than on thermal collectors. In PV modules, the solar cells are often connected in series. This way, one fully shaded solar cell will reduce the output of the whole string to zero. In the industry, this is known as the "Christmas-lights effect", referring to the way an entire string of series-strung Christmas tree lights will fail, if a single bulb fails. Bypass diodes can be used to mitigate this effect, by allowing current to flow in a different path, at the expense of a minor fraction of the total power [10]. In thermal collectors, the decrease in power produced due to shading is approximately proportional to the shaded area. Thus, shading clearly has a much bigger impact on PV panels than on thermal collectors.

3.3. Nomination of Cell String Configurations

Different cell string layout and configurations are evaluated searching for better performance in terms of the electrical output generated from the PVT. There are 38 cells in a string grouped in to 4 groups each group bypassed by a single bypass diode. The following nomination is used for the rest of the work.

- **3-16-16-3:** The solar cell string layout is shown in Figure 8. The cells are arranged as the figure, where the first bypass diode is in parallel to three (3) solar cells, the second bypass diode is in parallel with sixteen (16) solar cells, the third bypass diode is in parallel with sixteen (16) cells and the fourth bypass diode is in parallel with three (3) solar cells

Figure 8. 3-16-16-3 string of solar cells.

- **4-15-15-4:** The cells are arranged as follows: the first bypass diode is in parallel to four solar cells, second bypass diode in parallel with fifteen solar cells, third bypass diode in parallel with fifteen cells and the fourth bypass diode with four solar cells.
- **5-14-14-5:** The cells are arranged as follows: the first bypass diode is in parallel to five solar cells, second bypass diode in parallel with fourteen solar cells, third bypass diode in parallel with fourteen cells and the fourth bypass diode with five solar cells.

4. Theoretical Analysis

4.1. PV Cell Model

Photovoltaic energy is highly dependent on the environmental conditions, such as temperature and solar irradiation. Hence; the optimization of the energy conversion system is not a trivial problem. Solar cell modelling represents a current task, [1]. The analytical method, used to model the behaviour, the current I and terminal voltage V of a solar photovoltaic cell, is based on the use of the equivalent circuit for a photodiode. There are two model types for a solar cell. The single-diode and two diode model equivalent circuit approximation. The single diode model is widely used, being the respective solutions generally acceptable. For an ideal model, a PV device can be simply modelled by a *p-n* junction in parallel with a current source, which is associated to the photo generated carriers, I_{PV} (Figure 9 a). A more accurate model would take into account the influence of contacts and the leakage, by using series R_s and parallel R_p resistors, respectively (Figure 9 b).

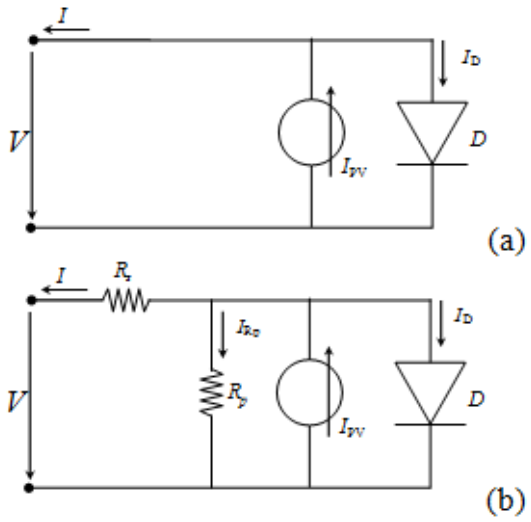

Figure 9. One diode model of solar cell: (a) Ideal PV cell model and (b) Real PV cell model

For an ideal PV cell:

$$I_{pv} = I_D + I \tag{2}$$

$$I_D = I_s\left\{\exp\left(\frac{qV}{nKT}\right)-1\right\} \tag{3}$$

$$I = I_{pv} - I_s\left\{\exp\left(\frac{qV}{nKT}\right)-1\right\} \tag{4}$$

$$I_{pv} = \left(C_o + C_1\Delta T\right)G. \tag{5}$$

Figure 10, shows the stationary $I(V)$ characteristic for a typical PV cell under different illumination (G) levels. It corresponds to the graphic representation of equations (4) and (5). The shaded area corresponds to the PV region.

For a real PV cell, taking the effect of contact and leakage resistances, the above equations are modified to the following:

$$I_{pv} = I + I_D + I_{Rp} \tag{6}$$

$$I_D = I_s\left\{\exp\left(\frac{qV + IR_s}{nKT}\right)-1\right\} \tag{7}$$

$$I_{Rp} = \frac{V + IR_s}{R_p} \tag{8}$$

$$I = I_{pv} - I_s\left\{\exp\left(\frac{q\left(V + IR_s\right)}{nKT}\right)-1\right\} - \left(\frac{V + IR_s}{R_p}\right) \tag{9}$$

where, I represents the current through the load, V the voltage across the load, I_{PV} is the light generated current, I_s is the diode leakage current in the absence of light, n is the ideality factor of the diode, q is the absolute value of the electronic charge, K is the Boltzmann constant, T is the absolute temperature, ΔT is the deviation of temperature from 25°C, R_s is the cell series resistance, associated with contact losses, R_{sh} is the shunt resistance, related to the leakage current of the device, C_o is a constant which depends on the solar cell area and characteristics, C_1 is the current dependence on temperature, and G is global irradiance.

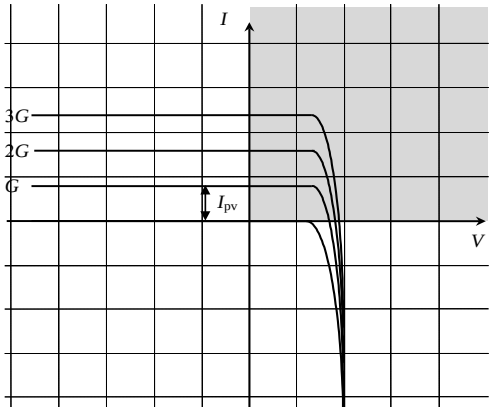

Figure 10. Stationary characteristic $I(V,G)$ of a PV cell under different illumination levels

Short circuit current, is obtained from equation (9), by setting V=0,

$$I_{sc} = I_{pv} - I_s\left\{\exp\left(\frac{q\left(I_{sc}R_s\right)}{nKT}\right)-1\right\} - \left(\frac{I_{sc}R_s}{R_p}\right) \tag{10}$$

Normally R_p>>Rs. Therefore, the last term in (10) can be neglected and, hence, is approximated by:

$$I_{sc} \approx I_{pv} - I_s\left\{\exp\left(\frac{q\left(I_{sc}R_s\right)}{nKT}\right)-1\right\} \tag{11}$$

In the ideal PV cell model R_S=0 hence, I_{sc}=I_{PV}.

The open circuit voltage V_{oc} is the voltage across the diode when the load current I =0A.

$$0 = I_{pv} - I_s\left\{\exp\left(\frac{q\left(V_{oc}\right)}{nKT}\right)-1\right\} - \left(\frac{V_{oc}}{R_p}\right).$$

The leakage resistance R_p is large and, as a result, the last term in above equation can be neglected. The open circuit voltage V_{oc} is approximated by,

$$V_{oc} \approx \frac{nKT}{q}\ln\left(\frac{I_{pv}}{I_s}+1\right). \tag{12}$$

The maximum power (P_{mp}) is given by

$$P_{mp} = I_{mp} \times V_{mp} \tag{13}$$

where, V_{mp} and I_{mp} are the voltage and current at maximum power point(MPP), respectively

Figure 11 shows the main features of solar cell or module.

Fill Factor (*FF*)

FF describes how close the *I-V* characteristics of solar cell are to the ideal characteristics; normally it is expressed as percentage.

$$FF = \frac{I_{mp} \times V_{mp}}{I_{sc} \times V_{oc}}. \tag{14}$$

Efficiency (η):

Solar cell electrical efficiency is given by

$$\eta_{el} = \frac{I_{mp} \times V_{mp}}{N \times A_{cell} \times G} \tag{15}$$

where, N is the number of solar cells and A_{cell} is the cell area

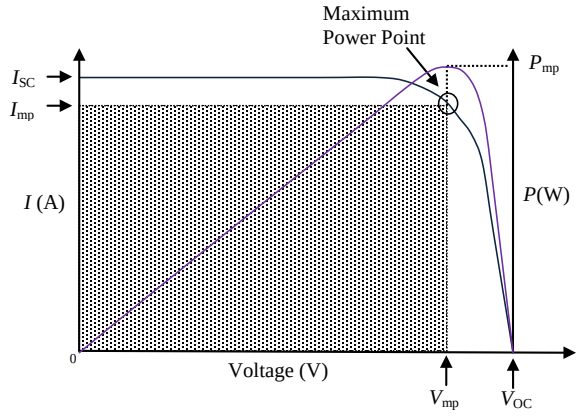

Figure 11. *I-V* and *P-V* curves of a photovoltaic cell/module

4.2. Shading in Solar Cells

Power generated by PV cells depends on solar irradiance, solar cell active area, cell conversion efficiency, temperature, etc. In a string of cells, the power reduction may be attributed to shading, mismatch effects, etc [11].

Partial shading greatly reduces the electrical energy generated from solar cells connected in series. If some of the cells are partially shaded, while others are illuminated, the current of the string will be limited by the worst performing cell, thus limiting the power generated by the string of cells. As per study carried in [12], the indoor solar laboratory tests showed that, shading a cell, parallel or perpendicular to the cell bus bar, had a similar impact in terms of power reduction. In terms of shading, for example when 25% of a cell is shaded, the power decrease is higher for the whole string. Interestingly to notice that, having 75% of all the solar cells in a string shaded or 75% of one solar cell, resulted in similar decrease in power. As expected, shading one whole (completely shaded) cell or string yields a very similar result, with the power output very close to zero. To prevent decrease in power and hotspot formation, PV panels include a bypass diode.

The maximum number of solar cells to be bridged by a bypass diode is determined by the reverse break down voltage (V_c) of the solar cells in the string. For an efficient operation, two conditions need to be fulfilled

1. bypass diode conducts when at least one cell is shaded;
2. the shaded cell voltage must stay at reverse voltage less than the reverse break down voltage (V_c).

Using the two conditions the maximum number (M) of solar cells to be bridged by a single bypass diode is,

$$M \le \frac{V_c - V_F}{V_{cell}} + 1 \qquad (16)$$

where V_F is the forward diode voltage and V_{cell} is the illuminated cell voltage.

5. Simulation Procedure and Results

5.1. Simulation Procedure

To achieve an easy manipulation of basic cell parameters and investigate their effect on the electrical characteristics of PV system, an efficient modelling of the solar cell is proposed using PSPICE simulator [13]. A single solar cell model is shown in Figure 12; it is used as a sub circuit for string of cells.

For simulation purposes some solar cell parameters are used as a starting point. The most important parameters are V_{oc}, I_{sc} and P_{mp}, which can be found from data sheet of PV cells. In a real solar cell, one diode model there are five parameters that are used to characterize the model. These are: the diode ideality factor (n), the reverse saturation current (I_s), the series resistance (R_s), the parallel resistance (R_p) and the photo generated current (I_{pv}). The values of R_s and R_p are assumed constant for specific value of illumination. The assumption will not much affect the conclusions [14].

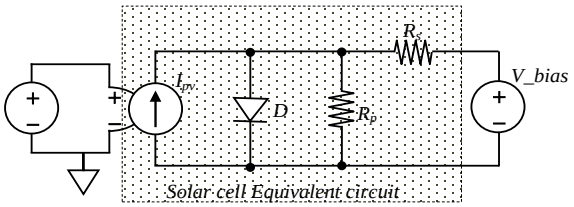

Figure 12. Equivalent circuit of solar cell in LTSPICE.

In order to characterize the basic unit of a photovoltaic cell, a SPICE sub circuit is adopted. The introduced sub circuit model specifies the photo generated current at an irradiance G, given by,

$$I_{pv} = \frac{J_{sc,ref} \cdot A_{cell} + C_1 \cdot \Delta T}{G_{ref}} \times G \qquad (17)$$

where, $J_{sc,ref}$ is the current density at STC (G_{ref} =1000W/m^2 and temperature 25°C), G is the solar irradiation at any instant, A_{cell} is the active area of a solar cell, C_1 is current dependence on temperature and ΔT is the deviation of temperature from 25°C. The specifications of solar cell used by Solarus are taken from data sheet. Namely, mono crystalline Si-solar cell (156mm×156mm), Isc=9.4A, V_{oc}=0.636V, P_{mp}=4.7W, I_{mp}= 8.9A, V_{mp}=0.534V and temperature coefficient (C_1) of I_{sc}=5mA/K.

$$J_{sc,ref} = \frac{9.4\text{A}}{0.156\text{m} \times 0.156\text{m}} \approx 390\text{A/m}^2.$$

Size of 1/3 cell size is (52×148) mm^2. So, I_{sc} at STC is:

$$I_{sc,ref} = 390\text{A/m}^2 \times (0.052\text{m} \times 0.148\text{m}) \approx 3\text{A}.$$

In case PV cells in a string are not uniformly illuminated, they generate different currents. The V_{oc} of a string is the sum of individual V_{oc} of all cells in the string.

5.2. Comparison of Simulation and Experimental Results

In Solarus two types of tests have being done, namely, the outdoor and solar simulator tests. A simulation was carried out to verify the results using LTSPICE simulation.

A. Outdoor test

Figure 13 shows a test receiver with 38 solar cells. Table 1 and Table 2 show data given from Solarus at outdoor test conditions of 5°C temperature and global irradiance G in comparison to simulation results.

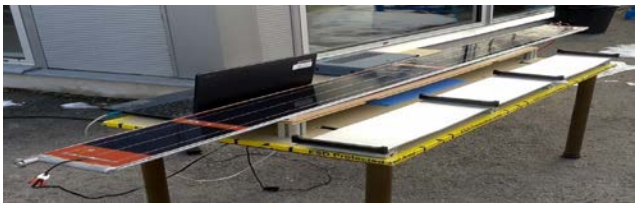

Figure 13. Outdoor test receiver 4-15-15-4 PV-cell string

Table 1. comparison of simulation and outdoor test results for G=800W/m^2 and temperature of 5°C

	Solarus data	Simulated	$\lvert\Delta_{abs}\rvert$	$\lvert\Delta_{rel}\rvert$%
G(W/m^2)	800	800	0	0
I_{sc} (A)	2.40	2.38	0.02	0.84
V_{oc} (V)	24.40	25.45	1.05	4.13
I_{mp} (A)	2.20	2.25	0.05	2.22
V_{mp} (V)	20.60	21.89	1.29	5.89
P_{mp} (W)	45.60	49.29	3.69	8.03
FF(%)	77.90	81.38	3.48	4.28
η_{cell}	20.30	21.07	0.77	3.66

where, $\lvert\Delta_{abs}\rvert$ is the absolute difference of simulated and outdoor test and $\lvert\Delta_{rel}\rvert$% is the percentage deviation from simulated results.

Table 2. Comparison of simulation and outdoor test results G=780W/m^2 and temperature of 5°C

	Data Solarus	Simulated	$\lvert\Delta_{abs}\rvert$	$\lvert\Delta_{rel}\rvert$%
G(W/m^2)	780	780	0	0
I_{sc} (A)	2.20	2.32	0.12	5.17
V_{oc} (V)	24.20	25.41	1.21	4.76
I_{mp} (A)	2.00	2.20	0.20	9.10
V_{mp} (V)	20.70	21.81	1.11	5.09
P_{mp} (W)	41.50	47.95	6.45	13.45
FF (%)	77.10	81.34	4.24	5.21
η_{cell}	18.90	21.02	2.12	10.09

The results from Solarus outdoor test and the simulation results show a good agreement. The deviations may be due to the accuracy related to the radiation meter used for the outdoor test

B. Solar simulator

The solar simulator results from Solarus were carried at a temperature of 5°C. A comparison of the results from solar simulator and simulated results are presented Table 3.

Table 3. Comparison of simulation and solar simulator test results, 1/3 test receiver with 38 Solar cells 4-15-15-4 #: weighted average of the Global irradiance G_{av}

	Data Solarus	Simulated	$\lvert\Delta_{abs}\rvert$	$\lvert\Delta_{rel}\rvert$%
G(W/m^2)	1889#	1889#	0	0
I_{sc} (A)	6.6	6.6	0	0
V_{oc} (V)	24.9	25.01	0.11	0.44
I_{mp} (A)	4.3	4.01	0.29	7.23
V_{mp} (V)	20.7	22.63	1.93	8.53
P_{mp} (W)	87.9	90.91	3.01	3.31
FF (%)	54.0	55.08	1.08	1.96
η_{cell}	-	16.46	-	-

Even though the solar simulator source is not a stable source, the data provided by Solarus and the results obtained by simulation are in a good agreement.

5.3. Prototype Circuit: Results AND Comparative Analysis

A circuit setup was tested as a prototype in Instituto Superior Técnico (IST) at Lisbon University (UL) to model the effects of shading and temperature. The circuit setup is represented in Figure 14. The diodes D_1 to D_{18} are plastic silicon rectifiers IN4003. With this experiment we intended to create an analogy with the effect of radiation on solar cell behavior. The current source associated to the illumination I_{PV} is replaced by a voltage source (V_1 to V_4) in series with a resistor of 1MΩ. This means that each voltage source V, expressed in volt, corresponds indeed to a current source expressed in microampere. V_5 is an adjustable DC voltage source connected in series with an ammeter. The setup consists of four groups of diodes, in a sequential arrangement of 2+5+5+2, each group having its own bypass diode across it. In order to change the current value, the voltage sources V_1, V_2, V_3, and V_4 are modified to meet the required current through each group of solar cells to demonstrate the shading effect.

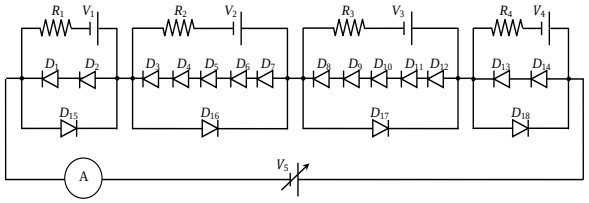

Figure 14. Circuit setup.

From now on, each example under analysis will be identified by the set of numbers I1-I2-I3-I4. For instance, the sequence 15-20-20-20 will represent the PV module with the first set of solar cells under a radiation associated to a current of 15μA and the remaining three have an illumination current of 20μA. The effect of temperature on the PV characteristics is also studied by placing the circuit assembly inside an oven for temperatures of 25°C and 40°C.

Comparison of simulation *vs* experimental results

The results presented correspond to the prototype, under different voltage (illumination) levels and temperatures (25°C and 40°C) in relation to those obtained by simulation in LTSPICE. Three situations are presented in Figure 15-Figure 17:

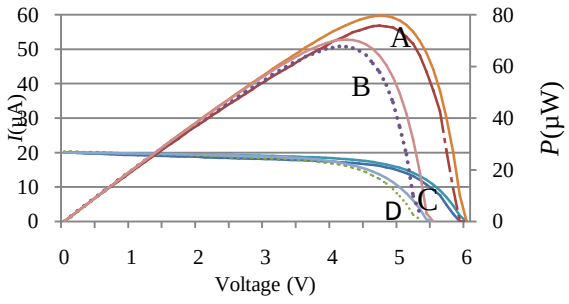

Figure 15. Experimental (broken line) and simulation (solid) results for 25°C (case A, *P-V* curve and case C, *I-V* curve) and 40°C (case B, *P-V* curve and case D, *I-V* curve), when the conditions are 20-20-20-20.

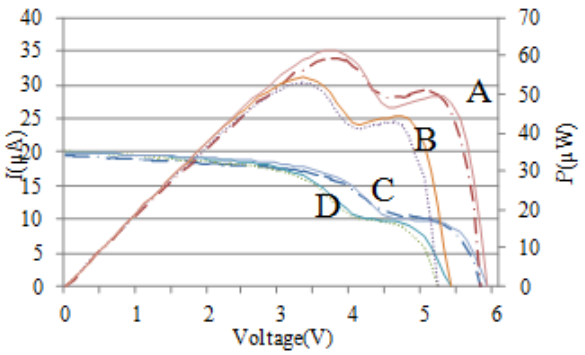

Figure 16. Experimental (broken line) and simulation (solid) results for 25°C (case A, *P-V* curve and case C, *I-V* curve) and 40°C (case B, *P-V* curve and case D, *I-V* curve), when the conditions are 10-20-20-20.

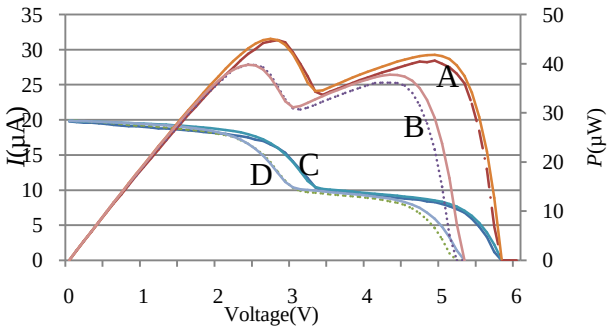

Figure 17. Experimental (broken line) and simulation (solid) results for 25°C (case A, *P-V* curve and case C, *I-V* curve) and 40°C (case B, *P-V* curve and case D, *I-V* curve), when the conditions are 20-10-20-20.

Results at room temperature are summarized in Table 4. The energy efficiencies are normalized to the value obtained for full uniform illumination conditions of the PV module.

Table 4. Experimental Vs simulation results, 25 °C

20-20-20-20				
	Simulation	Experimental	$\lvert\Delta_{abs}\rvert$	$\lvert\Delta_{rel}\rvert$%
V_{oc}	5.96 V	5.90V	0.06 V	1.00
I_{sc}	20.00 μA	20.00 μA	0 μA	0
V_{max}	4.70V	4.70V	0V	0
I_{max}	16.92 μA	16.10μA	0.82 μA	5.00
P_{mp}	79.50μW	75.67 μW	3.83 μW	5.00
FF	0.67	0.64	0.03	5.00
η_e	1	0.95	0.05	5.00
10-20-20-20				
V_{oc}	5.85V	5.80V	0.05V	1.0
I_{sc}	19.87 μA	19.40 μA	0.47 μA	2.00
V_{max}	3.70V	3.80V	0.10V	3.00
I_{max}	16.57 μA	15.60μA	0.97 μA	6.00
P_{mp}	61.30 μW	59.28 μW	2.02 μW	3.00
FF	0.53	0.53	0	0
η_e	0.78	0.77	0.01	1.00
20-10-20-20				
V_{oc}	5.80V	5.75V	0.05V	1.00
I_{SC}	19.87 μA	19.80 μA	0.07 μA	0.40
V_{max}	2.70V	2.80V	0.10V	4.00
I_{max}	16.69 μA	16.00 μA	0.69 μA	4.00
P_{mp}	45.10 μW	44.80 μW	0.30 μW	1.00
FF	0.39	0.39	0	0
η_e	0.57	0.57	0	0

The results show a remarkable agreement between experimental and simulated results, which ensures the model, can indeed be used as an important tool to the analysis of the main figures of merit related to the PV system.

5.4. Simulation Analysis Concerning Different Cell String Layout and Bypass Diode Configurations

The following simulations were carried to determine the effect of shading on the characteristics concerning different types of strings of 38 solar cells (1/3 cell type) produced by Solarus. The shading movement from one cell to the next following the sunrise may lead to a drastic change in the characteristics of the solar panel.

In the configuration reference the * sign indicates the group in which the solar cell affected by partial shading, and bridged by a bypass diode, is placed. For instance, in Figure 18, the denomination 3*-16-16-3 stands for a string of 38 solar cells with 4 bypass diodes in which at least one of the 3 solar cells bridged by the first bypass diode is affected by the frame's shade.

The 38 solar cells of the string are simulated as A) Without bypass diode; B) 3*-16-16-3; C) 4*-15-15-4 and D) 5*-14-14-5.

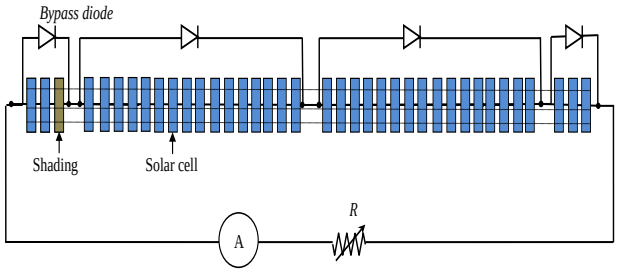

Figure 18. 3*-16-16-3 string layout

The results of the simulation results are presented below. Figure 19 shows, for different levels of shading, a histogram of the power generated by the PV module for the 4 strings of 38 cells previously referred as cases A, B, C and D. It is apparent from the graphic that:

- The configurations with bypass diode present clear advantageous in the power conversion process;
- the power generation is a decreasing function of the shading level;
- the best solution is case B, since it is the combination that corresponds to the minimum number of shaded solar cells for a given shading level.

Figure 20 shows the stationary *I-V* characteristic for case C at STC and for ten levels of shading percentage in steps $\Delta F = 0.1$. It is worth noticing the existence of 2 steps in the characteristic whenever shading is present ($F < 1$).

Figure 21 shows the *P-V* characteristic for case C considering STC and ten levels of shading percentage in steps $\Delta F = 0.1$.

One important detail is the presence of two power peaks (PP) whenever shading is present ($F < 1$). Let us refer them as primary and secondary MPP, for the peak power corresponding to the higher voltage and to the

smaller voltage, respectively. For small shading percentages (*F* near 1) the MPP is the primary. However, this one decreases quickly when *F* decreases, leading to a change of the MPP to the secondary MPP, which remains practically independent on *F*.

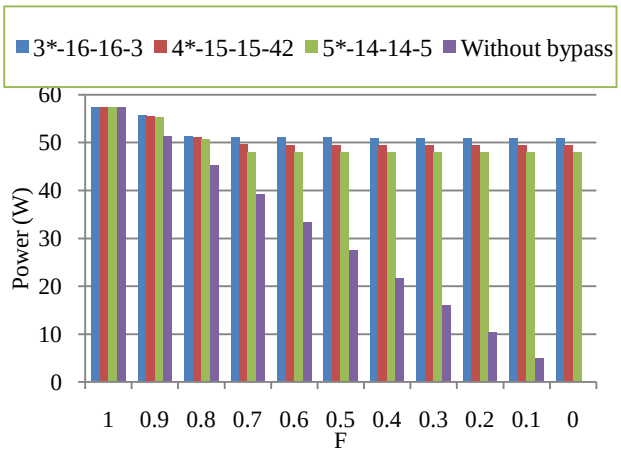

Figure 19. Power generated *vs* shading percentage

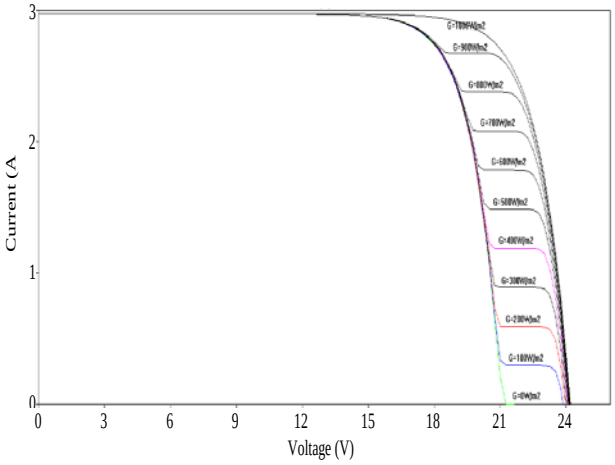

Figure 20. *I-V* curve (4*-15-15-4)

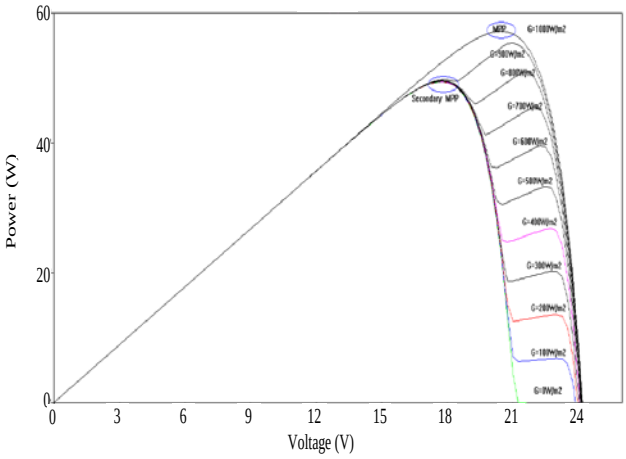

Figure 21. *P-V* curve (4*-15-15-4)

Similar simulation analysis where carried on when the shading affects the 2nd group of cells in the string for strings without bypass diode; 3-16*-16-3; 4-15*-15-4 and 5-14*-14-5.

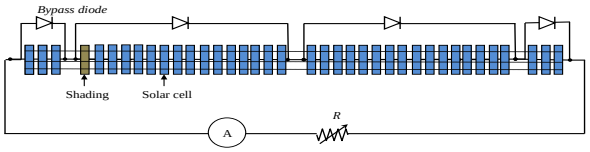

Figure 22. 3-16*-16-3 String layout

Figure 23 shows a histogram of the power generated by the PV module for the 4 strings of 38 cells previously referred.for different levels of shading. The conclusions are qualitatively similar to those referred for Figure 19, when the shading affected the 1st group of cells in the string. Quantitatively, there is a reinforcement of the negative effects associated to the shading, since the 2nd group bridged by the bypass diode has more cells than the 1st group.

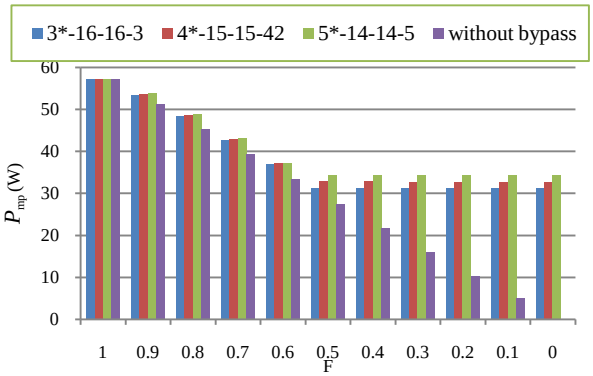

Figure 23. Power generated *vs* shading percentage

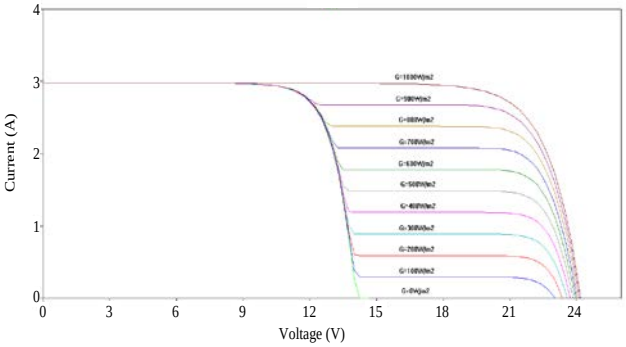

Figure 24. *I-V* curve (4-15*-15-4)

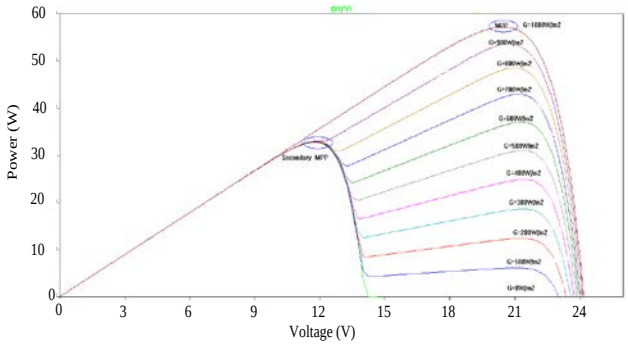

Figure 25. *P-V* curve (4-15*-15-4)

Figure 24 and Figure 25, show *I-V* and *P-V* characteristics for the string 4-15*-15-4. Comparing with Figure 21, it is apparent that the transition between the MPP is now reached for lower *F*: around 0.5 instead of

approximately 0.75, obtained for the string 4*-15-15-4. This may be explained by the fact that in the present case (4-15*-15-4) the shading effect is stronger and secondary MPP is lower (around 30W) than for the string 4*-15-15-4 (around 50W).

From the simulation results presented previously, the following conclusions are apparent

- when BP diodes are not included in the circuit, shading has greater effect on I_{sc}, P_{mp} and V_{oc};
- the inclusion of bypass diode mitigates the adverse reduction in the power generated. This is due to the presence of multiple peak power points in the presence of shading or non-uniform illumination.

6. Conclusion

It has been considered all along this work PV modules that are combinations of strings of solar cells manufactured by Solarus AB (38 cells and 4 bypass diodes).

Solar cell modelling and simulation in a PSPICE environment has been presented and validated by a comparative analysis of the associated results with those obtained in laboratory in IST and from Solarus AB. The effect of shading on the PV module has been analyzed. The results show a remarkable agreement with experimental data, which ensures that the simulation model can indeed be used as an important tool for the analysis of the main figures of merit related to the PV solar module. Moreover, the modelling can be used to define the solar cell string layout associated to different PV collector configurations in order to improve their performance accordingly with he defined requirements.

According to the obtained results, it is concluded that there is a substantial power loss due to non-uniform illumination or shading of solar cell strings. In shadow conditions, the decrease of the current in the branch where the PV cell is placed is proportional to the reduction in the irradiance. The bypass diode introduces a new peak in the *P-V* curve of the string characteristic, which may become the P_{mp} of the string, depending on the shading levels.

Even though, some simplifications have been introduced in the model and have clarified some aspects that should be relevant in the optimization of the performance of the PV solar panel. For instance, for all the available configurations of Solarus solar cell strings that have been simulated, when only one of the bypass diodes close to the frame is affected due to shading, the secondary P_{mp} will become the string P_{mp} when the illumination falls below 75%. Moreover, the P_{mp} reduction of the array will then remain constant, even if shadow levels increase. On the other hand, if one of the central bypass diodes is affected by shading, the new P_{mp} point will become the P_{mp} of the whole string if illumination falls below 50%. Another conclusion that should be referred is the following: no matter the configuration adopted for the Solarus strings, the bypass diodes maintain the P_{mp} reduction due to shading arising from the frame below 43%.

References

[1] Cubas J, Pindado S, de Manuel C. Explicit expressions for solar panel equivalent circuit parameters based on analytical formulation and the Lambert W-function. Energies, 2014, 7(7): 4098-4115.

[2] Acakpovi A, Hagan E B. Novel photovoltaic module modeling using Matlab/Simulink[J]. International Journal of Computer Applications, 2013, 83(16).

[3] V. Perraki, G. Tsolkas, "Temperature Dependence on the Photovoltaic Properties of Selected Thin-Film Modules", *International Journal of Renewable and Sustainable and Green Energy*, vol. 2, No. 4, pp. 140-146, 2013.

[4] *Solar cells*, chapter 2: Solar radiation, http://ocw.tudelft.nl/fileadmin/ocw/courses/SolarCells/res00026/CH2_Solar_radiation.pdf

[5] C. Giovinazo, L. Bonfiglio, J. Gomes, B. Karlsson, "Ray Tracing model of an Asymmetric Concentrating PVT", *International Solar Energy*, September 2014.

[6] Helgesson A. Optical Characterization of Solar Collectors form Outdoor Measurements. 2004.

[7] Adsten M. Solar Thermal Collectors at High Latitudes: Design and performance of non-tracking concentrators. Acta Universitatis Upsaliensis, 2002.

[8] https://www.jstage.jst.go.jp/article/jee/6/3/6_3_680/_pdf.

[9] R. Bernardo, H. Davidsson, N. Gentile, J. Gomes, C. Gruffman, L. Chea, C. Mumba, B. Karlsson, "Measurements of Electrical Incidence Angle Modifiers of an Asymmetric PVT CPC collector", Scientific Research 2012.

[10] C. Giovinazo, L. Bonfiglio, J. Gomes, B. Karlsson, "Ray Tracing model of an Asymmetric Concentrating PVT", *International Solar Energy*, September 2014,,

[11] Silvestre S, Chouder A. Effects of shadowing on photovoltaic module performance. Progress in Photovoltaics: Research and applications, 2008, 16(2): 141-149.

[12] Gomes J, Diwan L, Bernardo R, et al. Minimizing the impact of shading at oblique solar angles in a fully enclosed asymmetric concentrating PVT collector. Energy Procedia, 2014, 57: 2176-2185.

[13] R. Aloulou, P. de Peslouan, J. Armand , H. Minf, F. Alicalapa, M. Loulou, L. Luk, "Improved Circuit Model of Photovoltaic Cell for Energy Harvesting Application", 17th *IEEE Mediterranean Electro technical Conference*, Beirut, Lebanon, 13-16 April 2014.

[14] S. Kumar, "Shading Impact on Solar PV Module", *American International Journal of Research in Science, Technology, Engineering & Mathematics*, ISSN (Print): 2328-3491, ISSN (Online): 2328-3580, ISSN (CD-ROM): 2328-3629.